

Automated microscopy screening for compounds that partially revert cholesterol accumulation in Niemann-Pick C cells

Nina H. Pipalia,¹ Amy Huang,¹ Harold Ralph, Madalina Rujoi, and Frederick R. Maxfield²

Department of Biochemistry, Weill Medical College of Cornell University, New York, NY 10021

Abstract Niemann-Pick disease type C (NPC) is an autosomal recessive genetic disorder manifested by abnormal accumulation of unesterified cholesterol and other lipids. We screened combinatorially synthesized chemical libraries to identify compounds that would partially revert cholesterol accumulation. Cultured CHO cells with NPC phenotypes (CT60 and CT43) were used for screening along with normal CHO cells as a control. We developed an automated microscopy assay based on imaging of filipin fluorescence for estimating cholesterol accumulation in lysosomal storage organelles. Our primary screen of 14,956 compounds identified 14 hit compounds that caused significant reduction in cellular cholesterol accumulation at 10 μ M. We then screened a secondary library of 3,962 compounds selected based on chemical similarity to the initial hits and identified 7 compounds that demonstrated greater efficacy and lower toxicity than the original hits. These compounds are effective at concentrations of 123 nM to 3 μ M in reducing the cholesterol accumulation in cells with a NPC1 phenotype.—Pipalia, N. H., A. Huang, H. Ralph, M. Rujoi, and F. R. Maxfield. Automated microscopy screening for compounds that partially revert cholesterol accumulation in Niemann-Pick C cells. *J. Lipid Res.* 2006. 47: 284–301.

Supplementary key words high-content screening • filipin • lysosomal storage

Niemann-Pick disease type C (NPC) is an autosomal recessive genetic disorder that causes an abnormal accumulation of cholesterol and other lipids in many cell types (1, 2). The most serious symptoms are caused by progressive neuronal degeneration, but the liver and other peripheral organs also exhibit defects. Although the time course can be variable, symptoms often develop in early childhood, and the disease is usually fatal by the teens. There have been attempts to develop treatments for NPC (3–8), but no effective therapy exists at present.

Two genes have been linked to the NPC defect in humans, although the precise mechanisms of action of these proteins are still under investigation. NPC1 is a multispan

membrane protein that is typically associated with late endosomes or lysosomes (9), degradative organelles that hydrolyze cholesteryl esters brought into the cell via lipoproteins (10, 11). NPC1 has a sterol-sensing transmembrane domain that is similar to that found in endoplasmic reticulum proteins that respond to changes in cellular cholesterol (12). The NPC1 protein facilitates the transbilayer transport of some hydrophobic molecules, but it does not appear to transport cholesterol directly (13–16). NPC2 is a soluble luminal protein that is found in late endosomes and is able to bind cholesterol (17–19). NPC2 may shuttle free cholesterol (FC) to the limiting membrane of the late endosomes and lysosomes, where NPC1 apparently plays a role in its export to other cellular sites (20). Loss of functional NPC1 or NPC2 causes the accumulation of FC in endocytic organelles that have characteristics of late endosomes and/or lysosomes. These abnormal organelles will be referred to here as lysosome-like storage organelles (LSOs). The LSOs that are associated with NPC are quite similar to the LSOs associated with other hereditary glycosphingolipid storage disorders (often caused by the inability to metabolize a particular lipid) in that the storage organelles contain multilayered internal whorls of membrane bilayers that contain cholesterol, sphingomyelin, and high amounts of bis-(monoacylglycero)-phosphate (BMP), also known as lyso-bisphosphatidic acid (LBPA) (21, 22). Thus, even though these diseases arise from different genetic defects, certain aspects of the cellular phenotype are very similar.

Several lines of evidence indicate a defect in cholesterol transport in NPC, although defects in the transport of other lipids may also play an important role (23). NPC cells show abnormally high levels of unesterified

Abbreviations: BMP, bis-(monoacylglycero)-phosphate; DiI-LDL, low density lipoprotein labeled with C18-dialkyl-indocarbocyanine; FC, free cholesterol; LBPA, lyso-bisphosphatidic acid; LDH, lactate dehydrogenase; LSO, lysosome-like storage organelle; NPC, Niemann-Pick disease type C; PFA, paraformaldehyde; SCAP, sterol-regulatory element binding protein cleavage-activating protein; U18666A, 3- β -[2-diethylaminoethoxy]androst-5-17-one hydrochloride.

¹ N. H. Pipalia and A. Huang contributed equally to this work.

² To whom correspondence should be addressed.

e-mail: frmaxfie@med.cornell.edu

Manuscript received 26 August 2005 and in revised form 8 November 2005.

Published, JLR Papers in Press, November 15, 2005.

DOI 10.1194/jlr.M500388-JLR200

cholesterol, which accumulates mainly in the LSOs. The accumulation of cholesterol can be detected using filipin, a fluorescent detergent that binds to FC in membranes (24). In wild-type cells, excessive cholesterol delivered to cells from endosomes is either exported from the cell to extracellular acceptors or is esterified by ACAT, an enzyme localized in the endoplasmic reticulum (25). Despite the high content of FC in LSOs, the plasma membranes of NPC cells in culture actually have lower cholesterol content than normal cells (26) and a defect in cholesterol efflux to extracellular acceptors (27). Furthermore, there is a defect in the delivery of lipoprotein-derived cholesterol for esterification by ACAT (28, 29). All of these characteristics indicate that cholesterol efflux from late endosomes is grossly impaired in NPC cells.

Several different mutations are found in the NPC1 gene, which is responsible for ~95% of NPC disease in humans (13, 30–33). The correlation between the molecular defect and the age of onset of severe symptoms is unclear. The clinical presentation of NPC disease ranges from late onset or mild symptoms in adults to early onset with acute symptoms in infants (34, 35). This indicates that other factors in the genetic background can partially ameliorate the disease. Similarly, studies of cultured cells have shown that overexpression of various proteins that affect membrane traffic can reduce cholesterol accumulation. In particular, overexpression of the small regulatory GTPases, Rab7 and Rab9 (36–38), reduces sterol accumulation in cultured fibroblasts. Because these proteins regulate many aspects of cellular membrane traffic, they may not be good therapeutic targets. Nevertheless, the differences in the age of onset in humans and the effects of the overexpression of exogenous genes both indicate that pharmacological treatments might be developed to ameliorate symptoms even if the precise functions of the NPC proteins are not restored.

Many aspects of intracellular lipid and cholesterol transport are only partially understood (39–41). This makes it difficult to identify proteins that might be good targets for normalizing cholesterol transport in NPC cells. For this reason, cell-based screens that are unbiased in terms of protein targets are a good starting point. Such screens may lead to compounds that bind to novel target proteins that play a role in regulating cholesterol transport, possibly including compounds that could be developed into therapeutic agents that alter cholesterol metabolism. There has been one previous screen of a chemical library in cultured cells that had an NPC phenotype (5). One compound was found that corrected the NPC phenotype at micromolar concentrations, but it was toxic at concentrations close to the effective dose.

Recent advances in technology for high-throughput screens of cellular function have made it possible to develop novel assays to detect the effects of chemicals from libraries on cellular function. We have developed an automated microscopy assay for cholesterol accumulation in LSOs based on imaging of cell-associated filipin fluorescence. We screened a library of 14,956 combinatorially synthesized compounds on a CHO cell line with a NPC1

phenotype, CT60 (42), and identified 14 hit compounds that reduced cholesterol accumulation as assayed by filipin intensity at concentrations between 123 nM and 10 μ M. We selected a secondary library of 3,962 compounds chemically similar to these 14 compounds and identified 7 compounds that were effective at concentrations of <3 μ M. The effective compounds were also tested on a second CHO cell line expressing a different NPC1 mutation, CT43 (42), and several of the compounds had similar cholesterol-reducing effects on this cell line as well. Several of the compounds were effective at concentrations well below levels at which they were toxic to the cultured cells. These results show that we can implement a high-content screening method for cellular cholesterol content and distribution. Furthermore, potent compounds that alter cellular cholesterol distribution can be discovered using these methods.

METHODS

Materials

Cell growth media (Ham's F12 and Eagle's MEM with Earle's salts) as well as L-glutamine and FBS were purchased from Invitrogen (Carlsbad, CA). 3- β -[2-Diethylaminoethoxy]androst-5-17-one hydrochloride (U18666A) was from Biomol (Plymouth Meeting, PA). The compound library for screening was purchased from Chemical Diversity, Inc. (San Diego, CA). All other chemicals, including DMSO, filipin, paraformaldehyde (PFA), and Hoechst 33258, were purchased from Sigma Chemical (St. Louis, MO). Metamorph image-analysis software was from Molecular Devices (Downington, PA). Low density lipoprotein labeled with C18-dialkyl-indocarbocyanine (DiI-LDL) was prepared as described (43, 44).

Cell culture

The NPC1 cell lines CT60 and CT43 were provided by T. Y. Chang (Dartmouth Medical School, Hanover, NH). These cell lines are derived from the parental cell line, 25RA, which is a CHO cell line containing a gain-of-function mutation in the sterol-regulatory element binding protein cleavage-activating protein (SCAP) (42). Both CT60 and CT43 cells were grown in Ham's F12 supplemented with 1% penicillin/streptomycin, 2 g/l glucose, and 1.176 g/l sodium bicarbonate (medium A) containing 10% FBS in a humidified incubator with 5% CO₂ maintained at 37°C. For screening purposes, CT60 cells (650 cells/well) or CT43 cells (700 cells/well) in 30 μ l of growth medium A with 10% FBS were seeded on Costar 384-well black polystyrene flat, clear-bottomed tissue culture-treated plates (Corning, Inc., Corning, NY) to obtain ~80% confluence when cells were analyzed. For the study of LDL uptake, CT60 cells (4,000 cells/well) in 80 μ l of medium A with 10% FBS were plated on Costar 96-well special optics plates that have flat, ultrathin, polystyrene clear-bottom wells (Corning, Inc.).

Normal human fibroblasts (GM5659) were purchased from the Coriell Cell Repositories (Camden, NJ) and were grown in Eagle's MEM with Earle's salts, 2 mM L-glutamine, and 10% FBS. For microscopy, fibroblasts were plated in normal growth medium on glass-bottomed 35 mm dishes or on 384-well plates.

Screening

Compound addition. The library compounds were formatted for screening in the Rockefeller University High-Throughput

Screening Facility. Cells were treated with the compounds from the chemical library 1 day after plating. We added 0.1 μl of each compound (5 mM stock in DMSO) to 25 μl of screening medium S composed of medium A supplemented with 1% FBS and 20 mM HEPES on Falcon 384-well V-bottomed polypropylene plates using a Packard MiniTrak™ robotic liquid-handling system. To obtain $\sim 10 \mu\text{M}$ final concentration, 23 μl of the premixed compounds was dispensed onto the plates containing cells and 30 μl of culture medium A. For primary screening, 352 test compounds were added to each plate, and the remaining 32 wells were used as a control with only DMSO added. All plates were incubated with compounds for 16 h at 37°C. Plates were then washed three times with PBS, pH 7.4, using a Bio-Tek Elx405 plate washer (Bio-Tek Instruments, Inc., Winooski, VT). For each wash cycle, 70 μl of PBS was dispensed followed by aspiration with a residual volume of 16 μl /well. Finally, cells were fixed with 1.5% PFA in PBS for 20 min at room temperature, followed by three more washes with PBS.

Fluorescence labeling. To the fixed cells, filipin was added at a final concentration of 50 $\mu\text{g}/\text{ml}$ in PBS for 45 min at room temperature to label FC. Cells were finally washed three times with PBS, and images were acquired immediately after labeling.

Fluorescence microscopy. A Discovery-1 automatic fluorescence microscope from Molecular Devices equipped with a Xenon-arc lamp (Perkin-Elmer), a Nikon 10 \times Plan Fluor 0.3 numerical aperture objective, and a Photometrics CoolSnapHQ camera (1,392 \times 1,040 pixels; Roper Scientific, Tucson, AZ) was used to acquire images. Filipin images were acquired using 360/40 nm excitation and 480/40 nm emission filters with a 365 dichroic long-pass filter. The image files were stored on the local host computer before being transferred to a server.

Plates were transported from plate hotels using a CRS CataLyst Express robot (Thermo Electron Corp.). Images were acquired at two sites per well, each $\sim 50 \mu\text{m}$ from the center of the well, with 75 ms exposure time per image using 2 \times 2 binning. Automatic focusing was carried out by different methods for the primary and secondary screens. In the primary screen, each well was focused over a $\pm 150 \mu\text{m}$ range, and each site per well was focused over a $\pm 20 \mu\text{m}$ range using image-based focusing and the MetaMorph autofocus algorithm. Images for focusing were acquired with 15 ms exposure time using 8 \times 8 binning to reduce photobleaching. For the secondary screen, laser-based autofocus (LAF version 2 from Molecular Devices) was used to find the bottom of the plate. Image-based focusing was used to determine the offset between the bottom of the plate and the cells, and then each site was refocused over a 20 μm range. Acquisition time per plate was 60–75 min regardless of the focusing method. A total of 696 \times 520 pixel images were acquired at 12 intensity bits per pixel. Each pixel is 1.25 \times 1.25 μm in the object.

Image analysis. Images of filipin-stained cells were analyzed using Metamorph Discovery-1 image-analysis software. Two different image-analysis assays were developed: 1) the average filipin intensity assay, and 2) the LSO compartment ratio assay. First, to correct for shading, an image was created by averaging all of the images from a plate and smoothing the averaged image using a low-pass filter. Then, each pixel in an image was multiplied by the average intensity of the shading image, and the resulting pixel intensities were divided by the shading image on a pixel-by-pixel basis. Background was subtracted from each shading-corrected image by determining the fifth percentile intensity value of the image and subtracting this value from each pixel in the image. At the plating density used, all fields had at least 5% of the imaged

areas that were cell-free. Next, two different thresholds were applied to the filipin images. For the first, a low threshold was set to include all areas occupied by cells. The outlines of cells using the selected values were comparable to cell outlines in transmitted light images. A second, higher threshold was set for regions brightly stained with filipin in CT60 and/or CT43 cells, with the intention of mainly identifying the LSOs in the perinuclear region of the cells. For the average filipin intensity assay, using the low threshold alone, we measured total filipin intensity above the low threshold divided by the number of pixels above the lower threshold for each field. This gave an average filipin intensity per cell area. For the LSO compartment ratio, we measured the total filipin intensity selectively in the region above the higher threshold divided by the number of pixels in the lower threshold. This gave a measure of the total intensity of LSO filipin per cell area:

$$\text{Average filipin intensity} = \frac{\text{total intensity above low threshold}}{\text{number of pixels above low threshold}} \quad (\text{Eq. 1})$$

$$\text{LSO compartment ratio} = \frac{\text{total intensity above high threshold}}{\text{number of pixels above low threshold}} \quad (\text{Eq. 2})$$

Normalized values were obtained by dividing the values in the presence of each compound by the values obtained in the presence of the solvent control for each plate. Similar methods were used to analyze the effects of compounds on human fibroblasts treated with U18666A to induce cholesterol retention in LSOs.

Dose dependence. Using the same methods as for the screening, compounds were tested at 10 μM , 3.33 μM , 1.11 μM , 370 nM, and 123 nM in four wells each. Batches of selected compounds were purchased from Chemical Diversity, and 10 mM stocks in DMSO were made. A secondary stock plate of the 2 \times concentration (20 μM , 6.66 μM , 2.22 μM , 740 nM, and 246 nM) of the compounds was prepared in screening medium S. To obtain the final concentrations, 30 μl of this secondary stock was added to the cells in each well containing 30 μl of growth medium A supplemented with 10% FBS. The final DMSO concentration (0.1%, v/v) was the same in all wells. Cells were plated at 650 cells per well in 30 μl of growth medium A supplemented with 10% FBS on Costar 384-well plates. After 20 h of incubation in the presence of the compounds, cells were washed with PBS, fixed with PFA, and stained with filipin as described for the screening assay. Dose-dependence determination of the initial 14 hit compounds from the primary library was done at least five times in CT60 cells and three times in CT43 cells in separate experiments. Dose-dependence determination of the seven hit compounds from the secondary library was carried out at least three times in CT60 cells and two times in CT43 cells in separate experiments.

Time course assay. The effects of the compounds were determined at 1.11, 3.33, and 10 μM concentrations after 4, 20, and 48 h using methods similar to those used for dose dependence. The CT60 cells were seeded on three 384-well plates at 600 cells/well in growth medium on day 1. To maintain the same density of cells at the final time point, compounds were added chronologically. After overnight incubation, on the first plate (for the 48 h time point), compounds diluted in medium S were added in wells to achieve the final concentrations of 1.11, 3.33, and 10 μM . On the second plate, compounds were added in a similar manner 52 h after seeding the cells and allowed to incubate for 20 h. Finally, on the third plate, compounds were added 68 h after seeding the cells and allowed to incubate for 4 h. All three plates

were washed with PBS three times, fixed with 1.5% PFA, and stained with 50 $\mu\text{g/ml}$ filipin. Measurements were made from four wells for each condition in each experiment, and the experiments were repeated three times each for CT60 and CT43 cells. Images were acquired at 10 \times magnification on the Discovery-1 automatic fluorescence microscope for two sites per well and analyzed to obtain the LSO compartment ratio.

Cell count assay. Compounds were added to CT60 and CT43 cells plated on 384-well plates at 0 (DMSO solvent control), 5, 10, and 20 μM concentrations in quadruplicate using methods similar to those in the dose-dependence assay, except that the cells were stained with Hoechst 33258 nuclear stain. The final DMSO concentration in each well, including control wells, was 0.1% (v/v). The cells were incubated for 24, 48, and 72 h. After each time period, cells were washed with PBS, fixed with 1.5% PFA, and washed with PBS again. Nuclei were stained using 5 $\mu\text{g/ml}$ Hoechst 33258 (25 mg/ml stock solution in water) in PBS for 45 min at room temperature. Finally, cells were washed three times with PBS, and images were obtained using a Nikon 4 \times Plan Apo 0.2 numeric aperture objective. For Hoechst imaging, we used the same filter set as for filipin. We collected one 696 \times 520 pixel image per well at 12 intensity bits per pixel. Each pixel is 3.125 \times 3.125 μm in the object. Cells were counted by measuring the standard area of a single nucleus interactively for each plate using the Integrated Morphometry Analysis function of MetaMorph. The number of standard areas per object above a threshold was determined, and the total number of standard areas per image was used as the cell count. The percentage reduction in the number of cells compared with the DMSO control was calculated for each concentration and time.

LDL uptake. CT60 cells were grown in medium A to 70% confluence on 96-well special optics plates (Corning). After 24 h, DiI-LDL (6 $\mu\text{g/ml}$) and hit compounds (10 μM) in screening medium were added. In each experiment, eight wells per condition were used. After 18 h, cells were washed three times with PBS, fixed with 3% PFA for 20 min, and stained with 50 $\mu\text{g/ml}$ filipin for 75 min. Images were acquired using the Discovery-1 automatic fluorescence microscope at 20 \times magnification. DiI fluorescence images were acquired using a 535/40 nm excitation filter and a 610/60 nm band pass with a Chroma 51001 bs dichroic filter. Filipin was imaged as described above. Exposure time was 90 ms for filipin and 200 ms for DiI, and images were acquired at four sites per well with 2 \times 2 pixel binning. Three independent experiments were run. Images of both filipin and DiI were corrected for background and shading as described above. A low threshold was set to define the cell area based on filipin images, and the average DiI intensity was measured per cell area. Experimental data are presented as fractions of control values.

Lactate dehydrogenase cytotoxicity assay. The cytotoxicity of hit compounds was measured by a lactate dehydrogenase (LDH)-release assay kit according to the manufacturer's instructions (Roche Diagnostic GmbH, Penzberg, Germany) (45). CT60 cells were plated on Costar 96-well plates (Corning, Inc.) at a density of 3,500 cells/well and incubated for 24 h. Compounds were added to the CT60 cells at 0 (DMSO solvent control), 5, 10, and 20 μM concentrations in triplicate using methods similar to those in the dose-dependence assay. After 24 h of treatment, 100 μl of tissue culture supernatant was removed, and LDH activity was determined by measuring absorbance at 492 nm using a SpectraMax M2 fluorescence plate reader (Molecular Devices). The experiment was repeated three times, so averages from nine data points are reported.

Gas chromatography cholesterol assay. CT60 cells were plated on six-well plates in medium A supplemented with 10% FBS. After a 24 h incubation, cells were treated with 10 μM of each compound (10 mM stock in DMSO), medium A being replaced with medium A supplemented with 5.5% FBS and 20 mM HEPES. The change of the medium in the wells was performed to achieve experimental conditions similar to those used for the screening once chemical compounds were added to the cells. To control wells, only DMSO was added [0.1% (v/v) DMSO/well]. After 18 h of incubation at 37°C, cells were washed twice with HBSS. Cellular lipids were extracted with hexane-isopropyl alcohol (3:2, v/v) (46), dried under argon, resuspended in hexane, and separated on a gas chromatograph. A Hewlett-Packard gas chromatograph (model HP 5890 series II; Palo Alto, CA) equipped with a flame-ionization detector was used. A 15 m \times 0.53 mm HP-5 capillary column coated with 1.5 μm film thickness of 5% phenyl methyl siloxane was used to separate FC. The injection temperature was maintained at 255°C, and oven temperature was held isothermally at 260°C using helium as a mobile phase at a flow rate of 30 ml/min. The FC content of each well was quantified using β -sitosterol as the internal standard. After lipid extraction, cells were lysed with 0.1 M sodium hydroxide solution, and the protein content of each well (μg protein/well) was measured using a Bio-Rad DC protein kit (Bio-Rad Laboratories, Hercules, CA) that is based on the Lowry method (47). FC contents of compound-containing cells as well as control wells were normalized to the corresponding cellular protein. Experimental data are presented as fractions of control.

Immunofluorescence. CT60 cells were grown to 70% confluence on glass cover slip-bottom dishes. After 24 h, compounds were added (10 μM) to the cells in screening medium supplemented with 20 mM HEPES. After 16–22 h of compound treatment, cells were washed three times with PBS and fixed with 3.3% PFA for 20 min at room temperature. Cells were then treated with 50 mM ammonium chloride for 10 min and washed three times with PBS. After blocking with 0.1% BSA for 20 min, cells were washed with PBS, permeabilized with 0.05% saponin, and incubated with anti-LBPA/BMP (1:100) (a gift from J. Gruenberg, University of Geneva) (22) for 30 min at room temperature. Cells were washed three times with PBS and incubated with goat anti-mouse IgG-Alexa 546 (1:200) and 100 $\mu\text{g/ml}$ filipin for 30 min. Finally, cells were washed three times with PBS, and images were acquired on a Leica DMIRB microscope (Leica Mikroskopie und Systeme GmbH) equipped with a Princeton Instruments (Princeton, NJ) cooled charge-coupled device camera driven by MetaMorph Imaging System software. All images were acquired using an oil-immersion objective (25 \times , 1.4 numeric aperture). Anti-LBPA/BMP (IgG-Alexa 546) was imaged using a standard rhodamine filter cube, and filipin was imaged using a Leica A4 cube [360 nm (40 nm band pass) excitation filter and 470 nm (40 nm band pass) emission filter]. Images were analyzed using MetaMorph Discovery-1 image-analysis software to estimate cholesterol and LBPA content in the presence and absence of the compounds using the image-analysis algorithms as for screening.

RESULTS

Assay development

We developed assays for correction of the NPC phenotype in CHO cell lines using filipin, which binds to non-esterified cholesterol and has been used to visualize the FC content in NPC cells. Our initial screens were carried out

in CT60 cells, which express a mutated hamster NPC1 protein and a gain-of-function mutation in SCAP (42). These cells cannot traffic LDL-derived cholesterol out of late endosomes efficiently, and large amounts of cholesterol accumulate in LSO compartments. **Figure 1** shows images of filipin staining in a control CHO cell line, TRVb1 (48), and in CT60 cells. It can be seen that the CT60 cells show much more filipin staining than control cells and that the fluorescence in CT60 cells is concentrated in perinuclear LSO organelles.

For screening, images were acquired using a Discovery-1 automated microscopy system with a 10× objective and corrected for background and shading as described in Methods. Two thresholds were set for filipin staining: a low threshold to include all cell areas, and a high threshold for the strong filipin staining in the perinuclear LSOs. The threshold values were set for each plate from analysis of 64 images in 32 wells of untreated CT60 cells. It was found that the same thresholds could be used for multiple plates within an experiment, but the thresholds would vary among experiments conducted on different days. In developing the low threshold, we compared the outlines based on the thresholded cell images with transmitted light images, and the thresholds provided good agreement with the transmitted light cell boundaries.

As a simple measure of the intensity of filipin staining, we measured the filipin intensity per pixel above the threshold. The conditions of filipin labeling (time and concentration) were adjusted to optimize the discrimination between the CT60 cells and control TRVb1 cells. As shown in Fig. 1C, this simple method provided a reasonably high degree of discrimination between CT60 cells and TRVb1 cells. The quality of the assay for screening is expressed in terms of a statistical parameter, Z' (49):

$$Z' = 1 - [3\sigma_{c+} + 3\sigma_{c-}] / |\mu_{c+} - \mu_{c-}| \quad (\text{Eq. 3})$$

where σ_{c+} and σ_{c-} are the standard deviations of the positive and negative control data sets and μ_{c+} and μ_{c-} are the mean values of the positive and negative controls. The Z' value calculated using the average filipin intensity assay for the CT60 versus TRVb1 cells was 0.22, which is generally considered to be inadequate for large-scale screening because of the expected overlap of the two distributions when large numbers of wells are screened.

Although the intensity assay was potentially useful, it seemed that additional information in the images could provide better discrimination of wild-type versus NPC cells. For this purpose, we took advantage of the spatial distribution of the filipin labeling of the LSOs, which cluster near the nucleus (Fig. 1B). We applied the second, higher

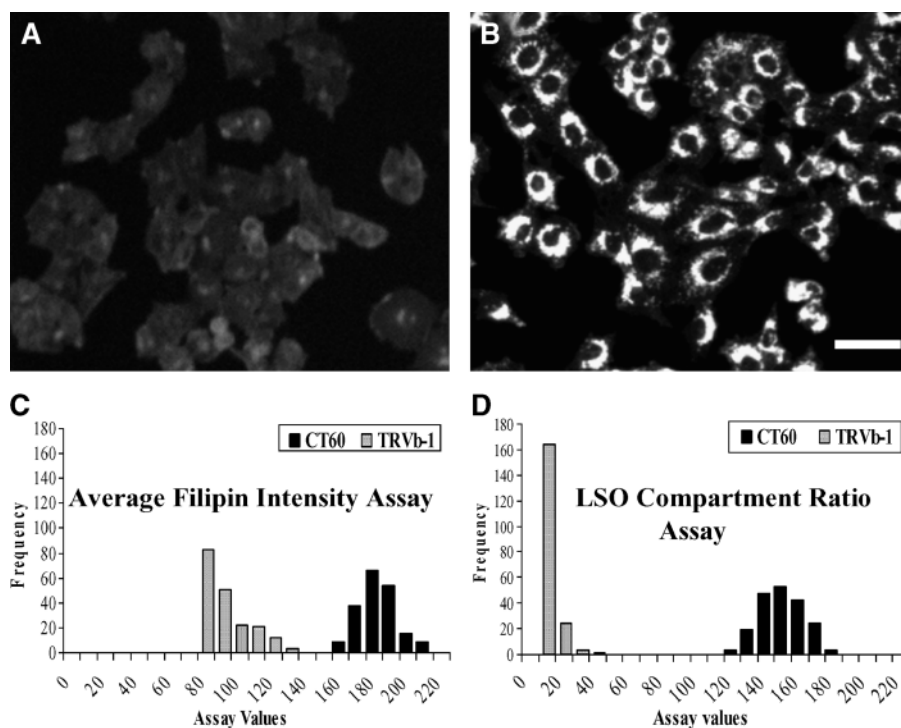


Fig. 1. Filipin labeling of cells. Wild-type CHO cells (TRVb1) and Niemann-Pick disease type C1 mutant CHO cells (CT60) were plated on 384-well plates and grown in regular growth medium for 48 h. Cells were washed with PBS, fixed with 1.5% paraformaldehyde (PFA), and stained with filipin. Images were acquired using the Discovery-1 automatic fluorescence microscope at 10× magnification for two positions per well using 360/40 nm excitation and 480/40 nm emission filters with a 365 dichroic long-pass (DCLP) filter. A: Filipin-stained image of TRVb1 cells. B: Filipin-stained image of CT60 cells. Bar = 30 μm. Images were analyzed using average filipin intensity and lysosome-like storage organelle (LSO) compartment ratio assays. C: Histogram of average filipin intensity values. D: Histogram of LSO compartment ratio values.

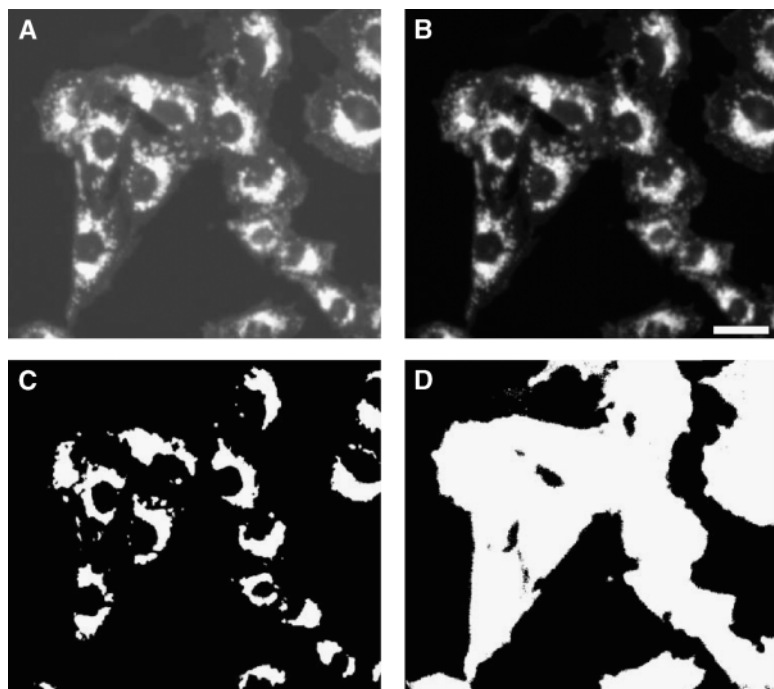


Fig. 2. Image-analysis method. Cells were fixed with PFA and labeled with filipin. A: Images acquired using the Discovery-1 automated fluorescence microscope at 10 \times magnification using 360/40 nm excitation and 480/40 nm emission filters with a 365 DCLP filter. B: Images after correction for shading and background. C: High-threshold setting used to identify the LSO compartment. D: Low-threshold setting used to include the entire cell area. Bar = 20 μ m.

threshold for this bright cluster. An example of the application of these thresholds is shown in **Fig. 2**. We then measured the total fluorescence intensity in the selected LSO objects (high threshold; **Fig. 2C**) divided by the total number of pixels in cells (low threshold; **Fig. 2D**). As shown in **Fig. 1D**, this LSO compartment assay gave a much stronger discrimination of the CT60 cells versus the control cells, with a Z' value of 0.61.

Chemical library screen

We screened a library of 14,956 compounds added to cells for 16 h at a final concentration of 10 μ M, using a single well for each compound. Before application of the compounds, cells were grown in normal tissue culture medium containing 10% FBS, so the LSOs were filled with cholesterol (**Fig. 1B**). The cells were then imaged and analyzed using the average filipin intensity assay and the LSO compartment assay. In general, the two analyses identified similar compounds that reduced the filipin labeling.

Wells that had average filipin intensities of >3 SD from the mean value of solvent-treated cells were examined further. Images from these selected wells were inspected visually, and sites that showed poor focus ($\sim 0.3\%$ of the total) were not reanalyzed if we had images from the second position. Wells that had a low number of cells were taken as an indication of toxicity, and these cytotoxic compounds were not pursued further. We also examined arrayed low-magnification images of rows and columns from the plates for patterns of cell number or brightness that might indicate a mechanical error in one of the automated pipetting steps. In one case, a banding pattern was seen in one set of eight plates, and these compounds were rescreened after fixing the pipetting problem.

From this initial screen, we found 133 compounds that reduced the average filipin intensity by >3 SD and 23 compounds that increased the average filipin intensity by >3 SD. Visual inspection of images also revealed 19 compounds that produced morphological changes in the

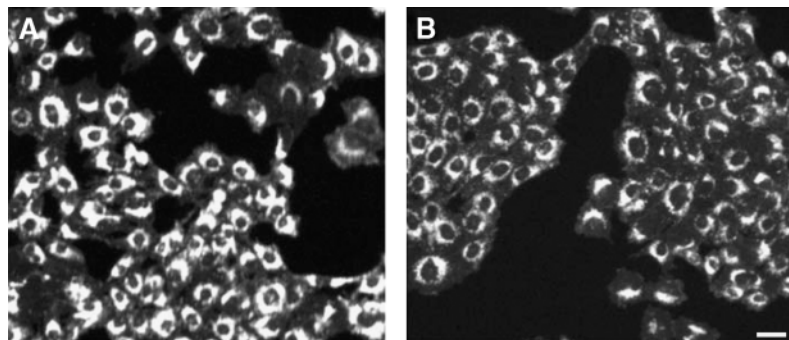


Fig. 3. Effect of a hit compound. CT60 cells were grown in growth medium overnight and treated with either solvent (A) or 10 μ M hit compound (1-a-13; B) in screening medium. After 20 h of incubation, cells were washed with PBS, fixed with PFA, and stained with filipin. Images were acquired at 10 \times magnification. Bar = 20 μ m.

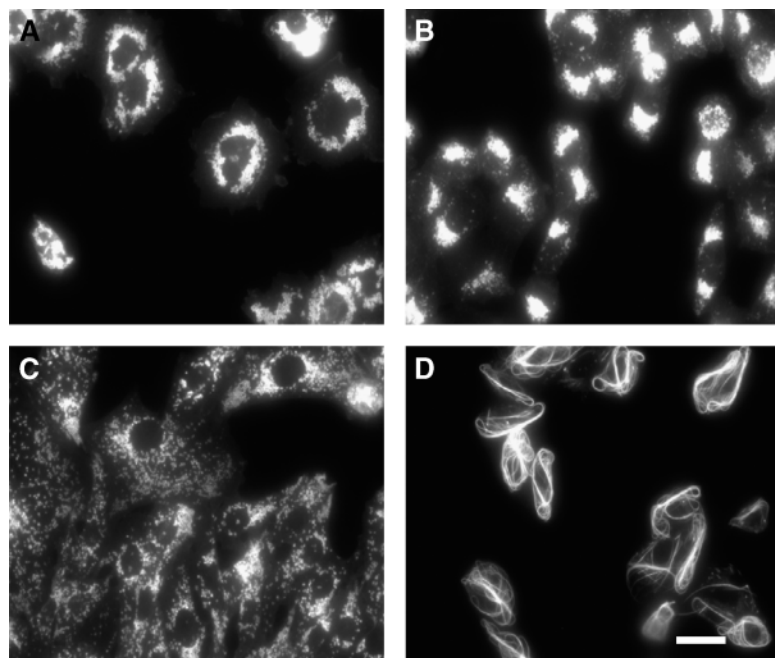


Fig. 4. Morphological changes induced by some compounds. A: Compound 1-c-1 resulted in more dispersed fluorescence with no significant change in average filipin intensity. B: Compound 1-c-2 induced more compact LSOs with no significant change in filipin intensity. C: Compound 1-c-3 caused perinuclear clusters of LSOs in mutant cells to become more dispersed. D: Compound 1-b-4 caused a significant increase in filipin intensity with filamentous or tubular staining. Bar = 15 μm .

filipin-staining pattern without meeting our criteria for reducing average filipin intensity.

These 175 compounds were then rescreened at 10 μM under the same conditions as the initial screen, except that each compound was placed in two wells per plate and duplicate plates were screened in parallel. Both the average filipin intensity and the LSO ratio values were determined. From the rescreening, 14 compounds were selected that reproducibly reduced filipin staining at 10 μM , and 8 compounds were found to reproducibly increase filipin staining. Nine compounds were found to alter the morphological distribution of filipin. **Figure 3** shows screening plate images of a solvent-treated control well and a compound-treated well showing decreased filipin staining.

Figure 4 shows the effects of four compounds that caused morphological changes as observed by filipin staining. These cells show rearrangements that may indicate that cholesterol has been redirected to a different compartment or that the morphology of the LSOs themselves has been changed (e.g., compound 1-c-3; **Fig. 4C**). The effect of compound 1-b-4 (**Fig. 4D**) was extremely dramatic, as bright swirls of filipin staining were observed. The effects of compound 1-b-4 were similar in normal human fibroblasts (data not shown), indicating that this response was not related to the NPC phenotype of the cells. The compounds that increased the apparent filipin staining and those that caused morphological changes were not investigated further in this study.

The structures of 14 compounds that decreased filipin staining, 2 that caused significant morphological changes (1-c-2, 1-c-3), and 2 that increased filipin staining (1-b-2, 1-b-4) are shown in **Fig. 5**. It can be seen that five of the hit compounds (1-a-5, 1-a-6, 1-a-7, 1-a-8, and 1-a-13) were from one synthetic family, and two (1-a-3 and 1-a-4) were from a second family.

Dose response

The effects of 14 hit compounds at various doses were examined, and the images were analyzed using both average filipin intensity and the LSO assay. **Figure 6A** displays the LSO compartment ratios at five concentrations (10, 3.33, 1.11, 0.37, and 0.12 μM) for CT60 cells. Three of the compounds reduced filipin staining by 3 SD below the solvent-treated mean at 1.1 μM in CT60 cells, and cells treated with these same compounds were >2 SD below the solvent-treated mean at 123 nM. Compound 1-a-14 has an unusual dose-response curve, which is probably associated with its cytotoxicity at higher concentrations. Two compounds, 1-a-9 and 1-a-10, did not show reproducible reductions in LSO compartment ratio, even though they were identified as hits during the screening process.

To determine whether the effects were specific to the CT60 cell line, we also tested the dose response of the 14 selected compounds on CT43 cells (**Fig. 6B**), another NPC1 mutant cell line derived from the parental cell line 25RA. Most of the compounds were effective at >3 SD below the untreated mean at 10 μM but lost their effect at lower concentrations on CT43 cells. It is interesting that the general trends of the effects of these 14 compounds are similar in both cell lines, although the compounds generally are more effective at a given dose in the CT60 cells.

Toxicity

To measure toxicity, we treated CT60 and CT43 cells with compounds at 5, 10, and 20 μM for 24 h. The cell number per well was compared with that of control cells treated with DMSO (**Fig. 7**). Many of the compounds did not cause a significant decrease in cell number at 10 μM after 24 h of incubation. Compound 1-a-14 did cause a

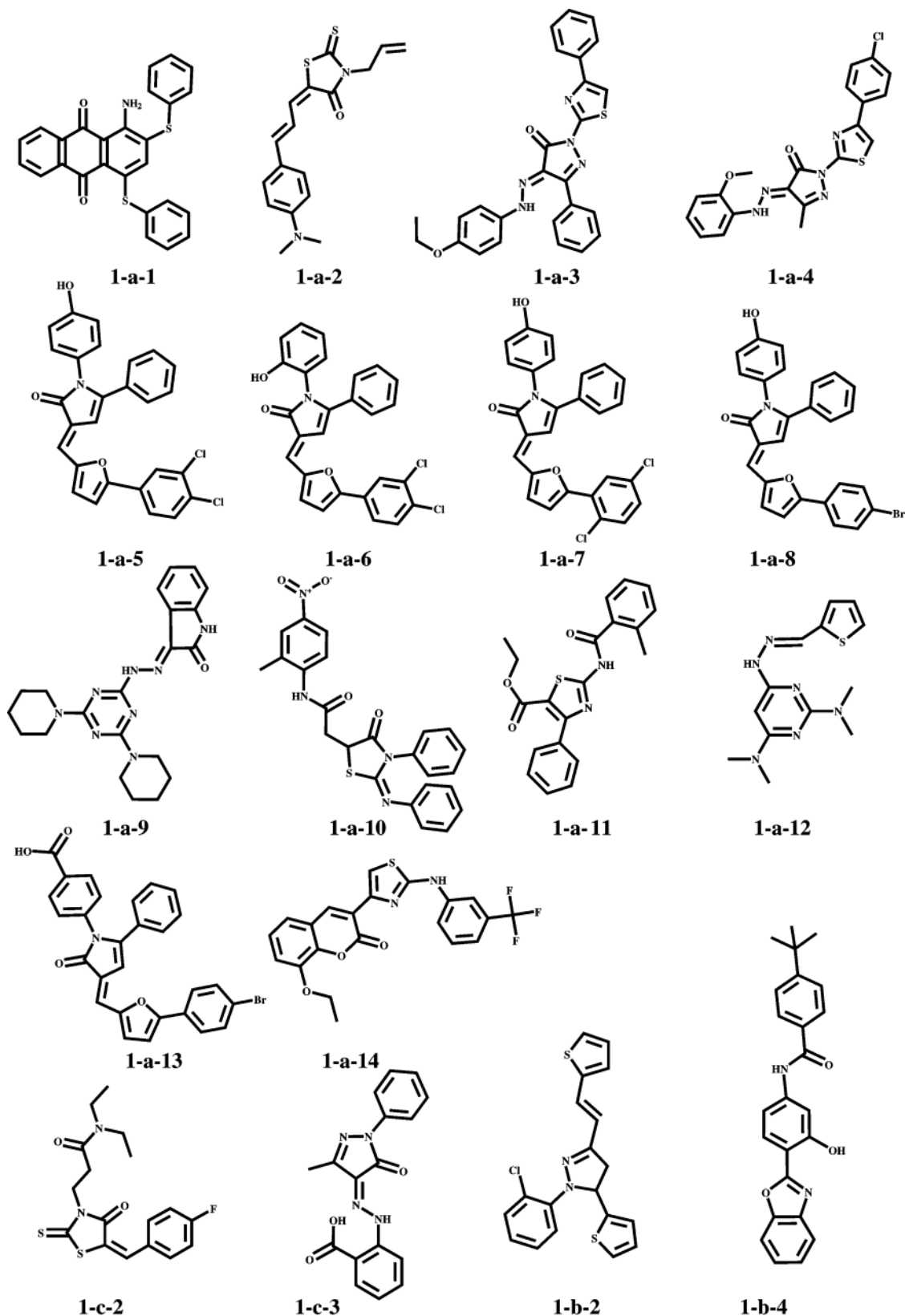


Fig. 5. Chemical structures of compounds from the primary library. The structures of the 14 hit compounds are shown. In addition, the structures of two compounds (1-c-2 and 1-c-3) that caused morphological changes, compound 1-b-2, which caused an increase in filipin intensity, and compound 1-b-4, which increased filipin intensity and induced morphological changes, are shown.

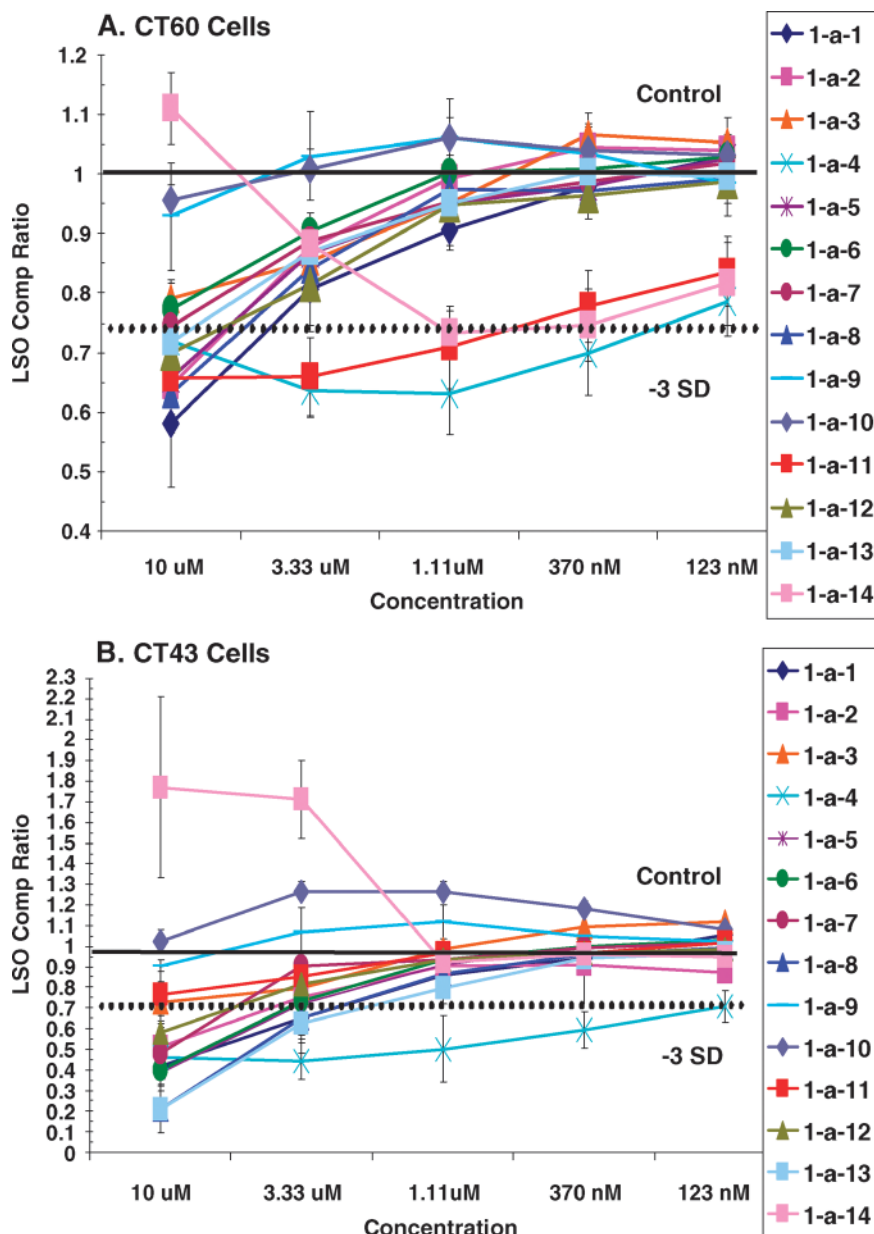


Fig. 6. Dose responses of 14 hit compounds from the primary library. CT60 and CT43 cells were seeded on 384-well plates in growth medium. After 24 h, compounds were added to achieve final concentrations of 123 nM, 370 nM, 1.11 μ M, 3.33 μ M, and 10 μ M in four wells per concentration, and cells were incubated overnight. Cells were then washed with PBS, fixed with PFA, and stained with filipin. The LSO compartment ratio was determined for CT60 cells (average of five experiments) (A) and CT43 cells (average of three experiments) (B). The solid horizontal lines indicate mean values for the solvent control, and the dashed lines indicate mean -3 SD. Error bars represent standard error.

50% reduction in cell number at 10 μ M for CT60 and an 80% reduction for CT43 cells. Compounds 1-a-4, 1-a-5, 1-a-6, 1-a-8, and 1-a-13 were partially toxic, as indicated by the 20–30% reductions in cell number after 24 h at 10 μ M.

Biochemical analysis of cellular cholesterol

The cholesterol-lowering effect of the 14 hit compounds identified by filipin labeling was measured by an alternative chemical method that involved GC separation of solvent-extracted cellular lipids (46). CT60 cells were

treated with compounds at 10 μ M under the same conditions used in the screening assays. Because the GC assay estimates FC content per cell, the values are compared with those from the average filipin intensity assay. As indicated in **Table 1**, most of the 14 hit compounds induce a relatively modest decrease of overall FC content of the cells, as measured by the average filipin assay. The hits from the first screen had variable effects on cellular cholesterol, including some compounds that apparently increased FC in the cells.

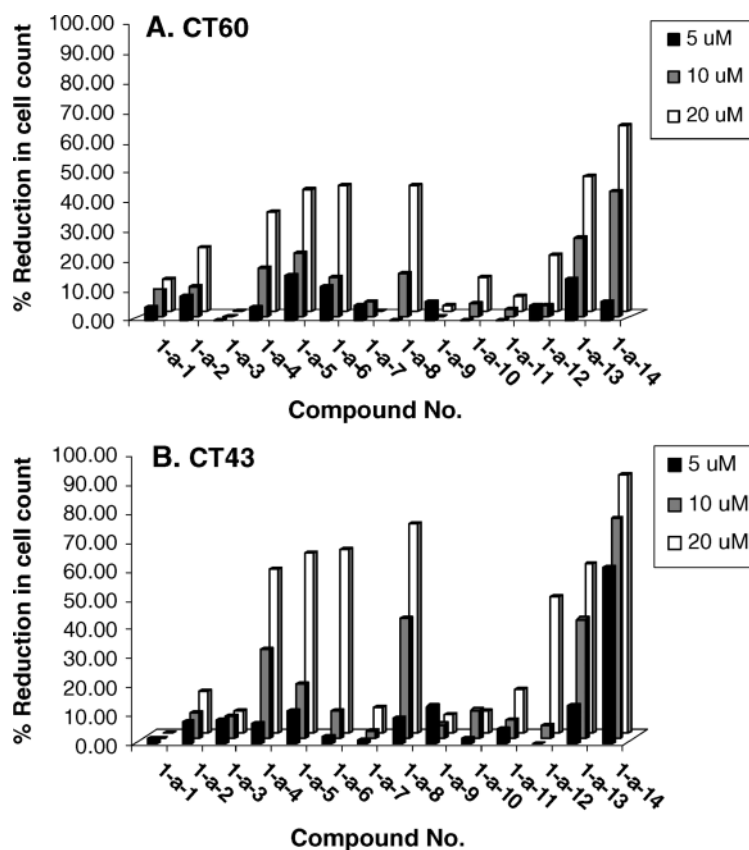


Fig. 7. Cytotoxic effects of 14 hit compounds from the primary library. CT60 and CT43 cells were seeded on 384-well plates in growth medium. After 24 h, compounds were added to achieve final concentrations of 5, 10, and 20 μM in four different wells per concentration, and cells were incubated for 24 h. An equivalent amount of DMSO was added in control wells. Cells were washed with PBS, fixed with PFA, and stained with the nuclear stain Hoechst 33258. Images were obtained at 4 \times magnification using the Discovery-1 automated fluorescence microscope with 360/40 nm excitation and 480/40 nm emission filters and a 365 DCLP dichroic filter. Cells per well were counted, and the percentage reduction in cell number compared with the control is shown for CT60 cells (average of four experiments) (A) and CT43 cells (average of three experiments) (B).

Secondary library

Based on the structures of the 14 hit compounds selected from the initial screen on CT60 cells, we purchased a secondary library of 3,962 compounds from the initial supplier. The compounds were selected based upon the chemical similarity in terms of the Tanimoto coefficient (50).

We performed a screen of these 3,962 compounds using a protocol similar to the primary library screen, except that compounds were initially screened at two concentrations, 10 and 1 μM . Each compound was added in a single well, and images were acquired for two positions per well and averaged to give a single value. Two full screens of the secondary library were carried out at both concentrations. The images were analyzed using both the average filipin intensity and the LSO compartment ratio methods. At 10 μM , we found 574 compounds that were 3 SD below controls as determined by one of the analysis methods and 34 compounds that were 3 SD below controls by both of the analysis methods. At 1 μM , we found 202 compounds that were 3 SD below controls by at least one of the analysis methods and 6 compounds that were 3 SD below controls by both methods.

We cherry-picked these 202 compounds and rescreened them twice at 1 μM , 300 nM, and 100 nM. We added each compound to four different wells at each concentration, and measurements from images at two positions per well were averaged. With the two screens, we obtained eight values by each analysis method for every compound at 1 μM , 300 nM, and 100 nM. Together, we had 10 values (2 from the first screen and 8 from the cherry-picking

round) for 1 μM and 8 values for 300 and 100 nM for each analysis method (average filipin intensity and LSO compartment ratio). Based on these data, we selected seven compounds for further analysis, and their chemical structures are shown in **Fig. 8**.

The dose-response curves for the seven selected compounds are shown in **Fig. 9**. The data indicate that four compounds (2-a-8, 2-a-9, 2-a-12, and 2-a-13) showed a >3 SD reduction in the LSO compartment assay at 370 nM,

TABLE 1. FC content by average filipin intensity and GC assays for CT60 cells treated with 14 hit compounds from the primary library

Compound	Average Filipin Intensity	$\mu\text{g FC}/\mu\text{g Protein}$ by GC
1-a-1	0.87 ± 0.03	1.02 ± 0.03
1-a-2	0.88 ± 0.01	1.15 ± 0.05
1-a-3	0.95 ± 0.03	1.27 ± 0.07
1-a-4	1.01 ± 0.03	0.87 ± 0.07
1-a-5	0.89 ± 0.03	1.18 ± 0.06
1-a-6	0.92 ± 0.02	1.37 ± 0.01
1-a-7	0.89 ± 0.02	1.04 ± 0.13
1-a-8	0.90 ± 0.02	1.31 ± 0.10
1-a-9	0.99 ± 0.06	0.86 ± 0.07
1-a-10	0.96 ± 0.02	1.23 ± 0.08
1-a-11	0.90 ± 0.03	0.82 ± 0.07
1-a-12	0.91 ± 0.03	0.73 ± 0.03
1-a-13	0.97 ± 0.07	1.54 ± 0.11
1-a-14	1.24 ± 0.10	1.44 ± 0.16

FC, free cholesterol. FC content of CT60 cells was measured by a screening method (average filipin intensity assay) and by gas chromatography after incubation with 10 μM of 14 hit compounds from the primary library for 20 h. Data are presented as fractions of solvent-treated controls.

and three compounds (2-a-8, 2-a-9, and 2-a-12) also showed an effect 2 SD below solvent control at 123 nM on CT60 cells. As with the hits from the first round, most of these compounds were also effective on CT43 cells (Fig. 9B).

We measured LDL uptake under conditions similar to the screening conditions by incubating cells with DiI-LDL during the incubation with compounds. As shown in **Table 2**, all of the hit compounds from the secondary library, except 2-a-15, caused a decrease in LDL uptake during an 18 h incubation. It will require further work to determine whether this is a primary effect of some of the compounds or whether the decrease in LDL uptake is

secondary to the release of cholesterol from the LSOs. Although CT60 cells have a partial defect in SCAP function as a consequence of a point mutation in one SCAP allele (51, 52), it would be expected that the cells would respond to increased cholesterol by decreasing the expression of LDL receptors.

Figure 10 shows the results of a toxicity assay on the seven hit compounds from the secondary library. Compound 2-a-12 caused an $\sim 40\%$ reduction in cell count at 10 μM after 24 h for both CT60 and CT43 cells. Hence, this compound was eliminated from further evaluation by biochemical methods. The other compounds caused either no loss of cells or only a slight loss under the con-

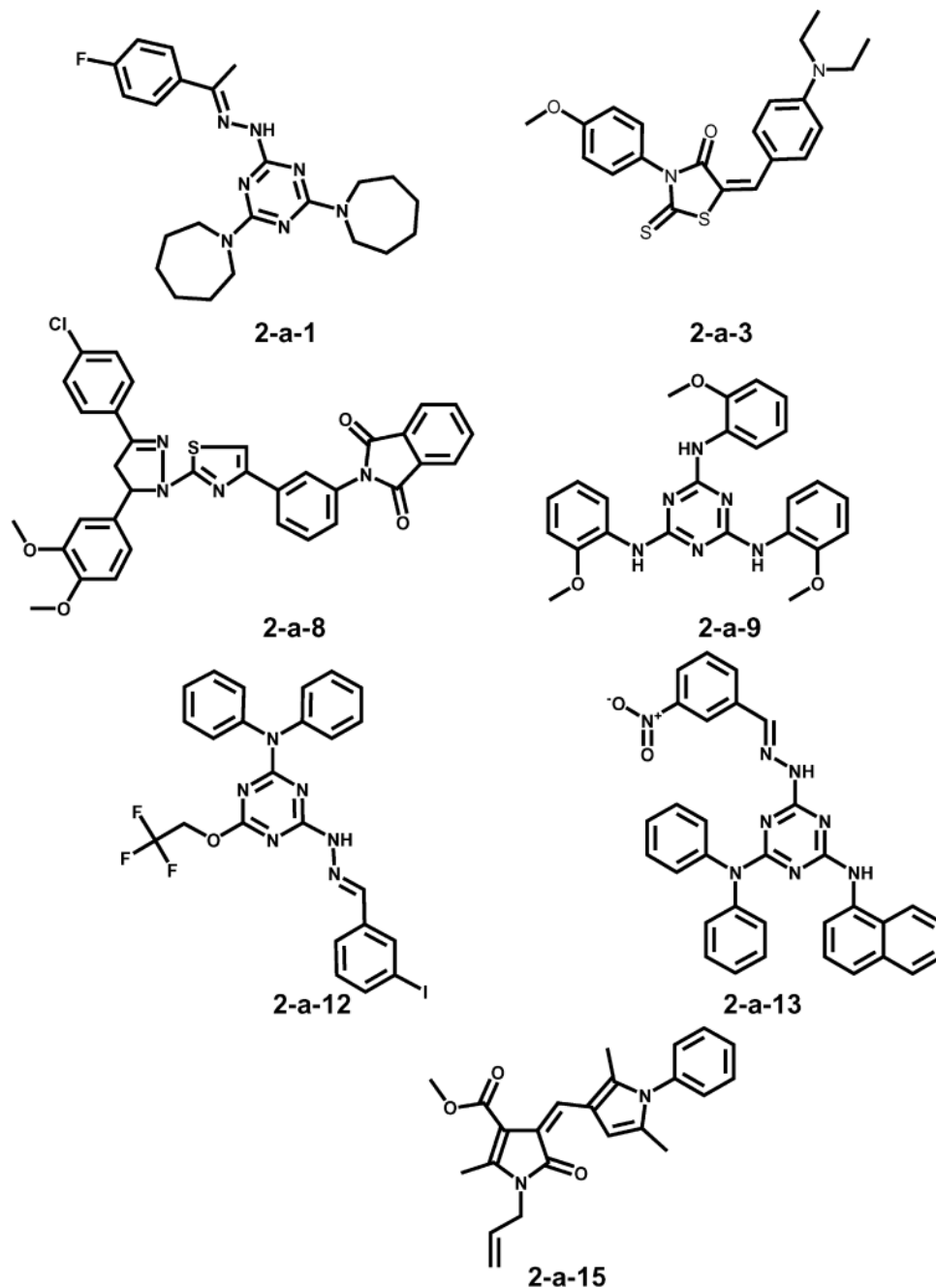


Fig. 8. Chemical structures of seven hit compounds from the secondary library.

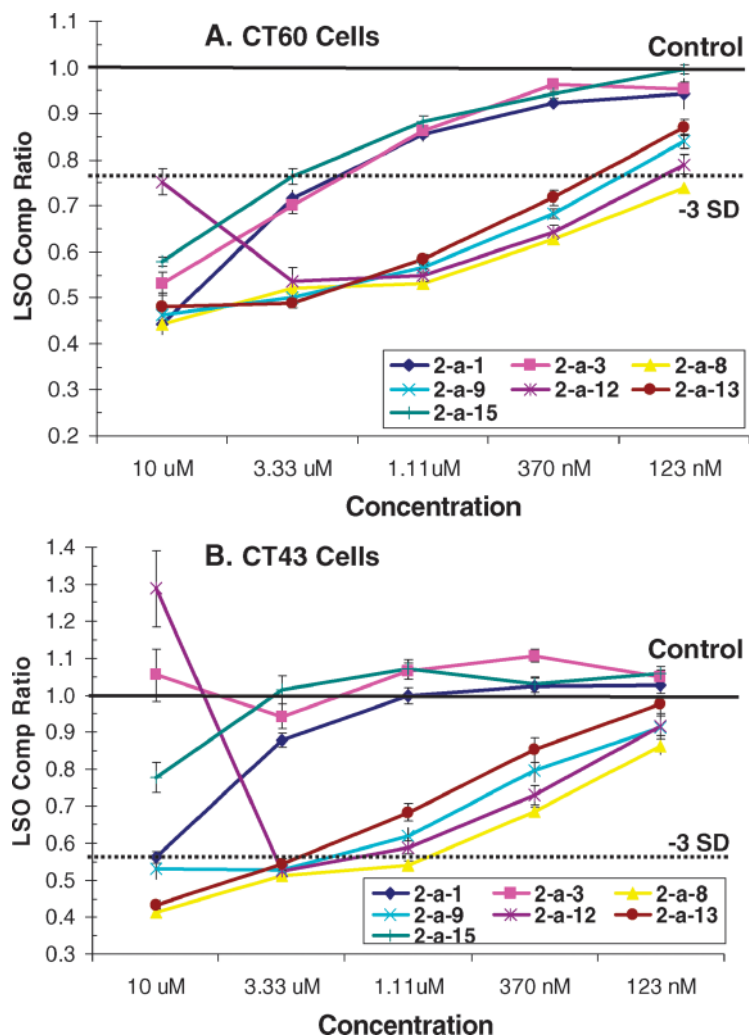


Fig. 9. Dose dependence of seven hit compounds from the secondary library. The dose dependence was determined as described for Fig. 6 for the seven hit compounds from the secondary library for CT60 cells (average of five experiments) (A) and CT43 cells (average of three experiments) (B). The solid horizontal lines indicate mean values for the solvent control, and the dashed lines indicates mean $- 3$ SD. Error bars represent standard error.

ditions in which they reduced filipin staining. We also analyzed the cytotoxicity of these compounds by LDH release into the medium (45). As shown in Fig. 10C, the cytotoxicity measured by this assay was less than the reduction in cell count, indicating that the compounds may have slowed cell growth without causing cell death after 24 h.

The time course of the reduction in the LSO compartment ratio at 1.1, 3.3, and 10 μ M is shown in Fig. 11. After a 4 h treatment, compound 2-a-3 showed a >3 SD decrease in LSO compartment ratio at 10 μ M. After 20 h, all of the compounds showed a reduction in LSO compartment ratio at 10 μ M, and several compounds were effective at 1.11 and 3.33 μ M. After the 48 h treatment, the effectiveness in reducing LSO compartment ratio was generally retained.

The decrease of cellular cholesterol upon treatment with the selected compounds was measured by GC analysis (Table 3). In contrast with the results from the primary library, all of the hit compounds from the secondary library reduced cellular cholesterol as measured biochemically. These compounds also generally showed a lower value for the average filipin intensity assay than the hit compounds from the primary library.

Effects of compounds on normal human fibroblasts treated with U18666A

All of the results described above were obtained with CHO cells that have a mutation in SCAP in addition to their mutations in NPC1. To determine whether the compounds might have effects on other types of cells, we treated normal

TABLE 2. DiI-LDL uptake by CT60 cells treated with seven hit compounds from the secondary library

Compound	DiI Intensity/Cell Area
2-a-1	0.43 \pm 0.01
2-a-3	0.62 \pm 0.01
2-a-8	0.77 \pm 0.01
2-a-9	0.85 \pm 0.01
2-a-12	0.72 \pm 0.01
2-a-13	0.72 \pm 0.01
2-a-15	1.00 \pm 0.01

DiI-LDL, low density lipoprotein labeled with C18-dialkyl-indocarbocyanine. Cells were incubated with DiI-LDL (6 μ g/ml) in the presence of compounds (10 μ M) for 18 h. The DiI intensity per unit of cell area was measured as described in Methods. Values are normalized to the intensity per cell area for control (solvent-treated) cells. Data are presented as fractions of solvent-treated controls \pm SEM based on averages from three experiments with 32 images from eight wells analyzed for each condition per experiment.

human fibroblasts with compound U18666A, which induces cholesterol accumulation similar to that seen in NPC cells (53). We found that treatment of cells with 250 or 500 nM U18666A for 20 h caused a significant increase in cholesterol accumulation, as seen by filipin staining (data not shown) and as measured by the LSO compartment ratio method (Fig. 12). When cells were treated with hit

compounds from the secondary library, several of these compounds caused a significant decrease in filipin staining (Fig. 12). In particular, compound 2-a-1 caused a dramatic decrease in filipin staining.

DISCUSSION

We have developed and applied an automated screening protocol to identify compounds that partially reverse the phenotype of NPC mutant cells. The screen is based on the binding of a fluorescent detergent, filipin, to FC. In the untreated mutant cells, there is a large amount of FC compared with that in control cell lines (42). This cholesterol is highly concentrated in LSOs, organelles that are related to late endosomes, but they also contain protein markers that are usually not abundant in late endosomes (54). The molecular defect in NPC is a mutation or absence of one of two proteins associated with late endosomes, NPC1 and NPC2. These mutations cause a defect in the efflux of cholesterol from late endosomes, resulting in high levels of cholesterol accumulation in the LSOs. Our current studies were focused specifically on NPC1 mutations.

We used an automated microscopy, high-content analysis approach for the screens, and two screening procedures were analyzed. In the first procedure (average filipin assay), we used a simple threshold to identify the areas in each image that contained cells, and we measured the total fluorescence power above the threshold in each field. The intensity of staining of the plasma membrane was sufficient to provide a good distinction of cellular areas above background, and the identified cellular areas were not highly sensitive to the choice of threshold value. The assay parameter that was used was the total fluorescence power divided by the number of pixels above threshold. This assay was designed to roughly correlate with the total cholesterol per cell. This is based on the approximation that cell area is constant under various conditions, which will not be true if cells spread or round up significantly in response to a treatment. Rounding up, which is often caused by toxicity, will increase this parameter, so it would not lead to false-positives in our search for compounds that decrease FC.

The assay also depends on the ability to measure FC by filipin staining. Although filipin intensity increases as FC levels increase, it is possible that some pools of cholesterol will differ in their ability to bind filipin. Also, it is possible that some treatments might interfere with filipin binding and thereby decrease filipin staining without actually reducing cholesterol levels. For that reason, we used a chemical assay of cholesterol content. As shown in Table 3, several of the compounds from our secondary library decreased cellular cholesterol as measured by GC, in agreement with the changes in the average filipin assay value. In the first library (Table 1), we generally found modest decreases in the average filipin values, and we did not find lower cholesterol in the chemical assay.

Although the average filipin assay did not use subcellular information or single cell analyses, it benefited from

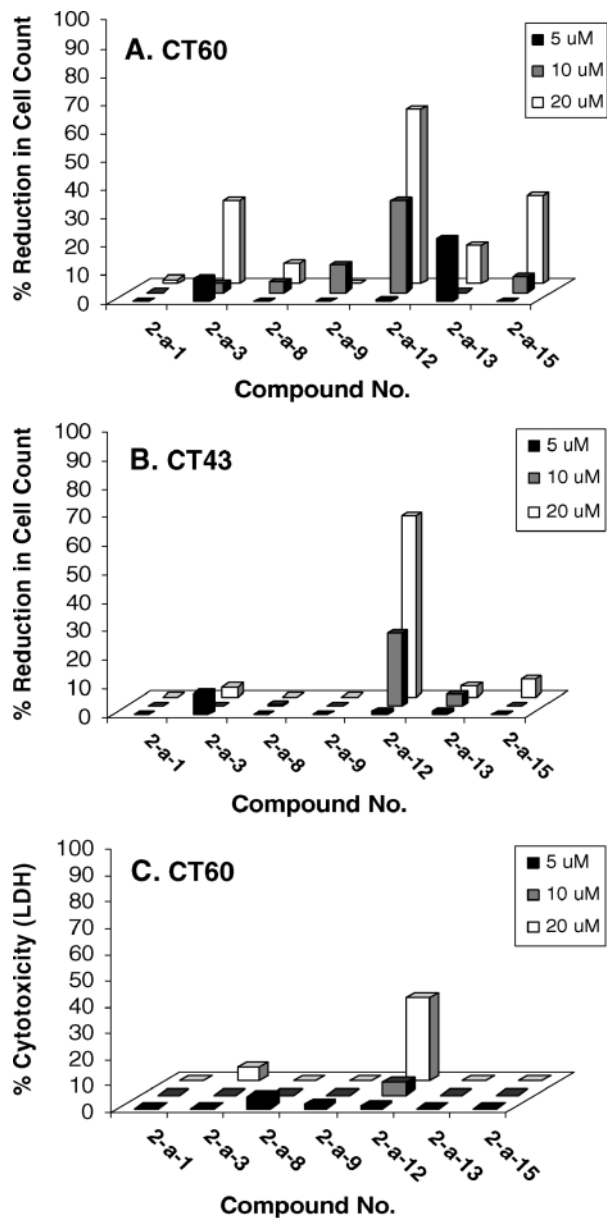


Fig. 10. Cytotoxic effects of seven hit compounds from the secondary library. Cytotoxicity was measured by cell count and by lactate dehydrogenase (LDH) release for the seven hit compounds from the secondary library. For cell count assays, cells per well were counted as described for Fig. 7, and the percentage reduction in cell number compared with the control was determined for CT60 cells (A) and CT43 cells (B). For the LDH cytotoxicity assay, the percentage of cellular LDH released into the medium was measured in the presence of seven hit compounds from the secondary library for CT60 cells with reference to low (no compounds) and high (lysed cells) controls (C).

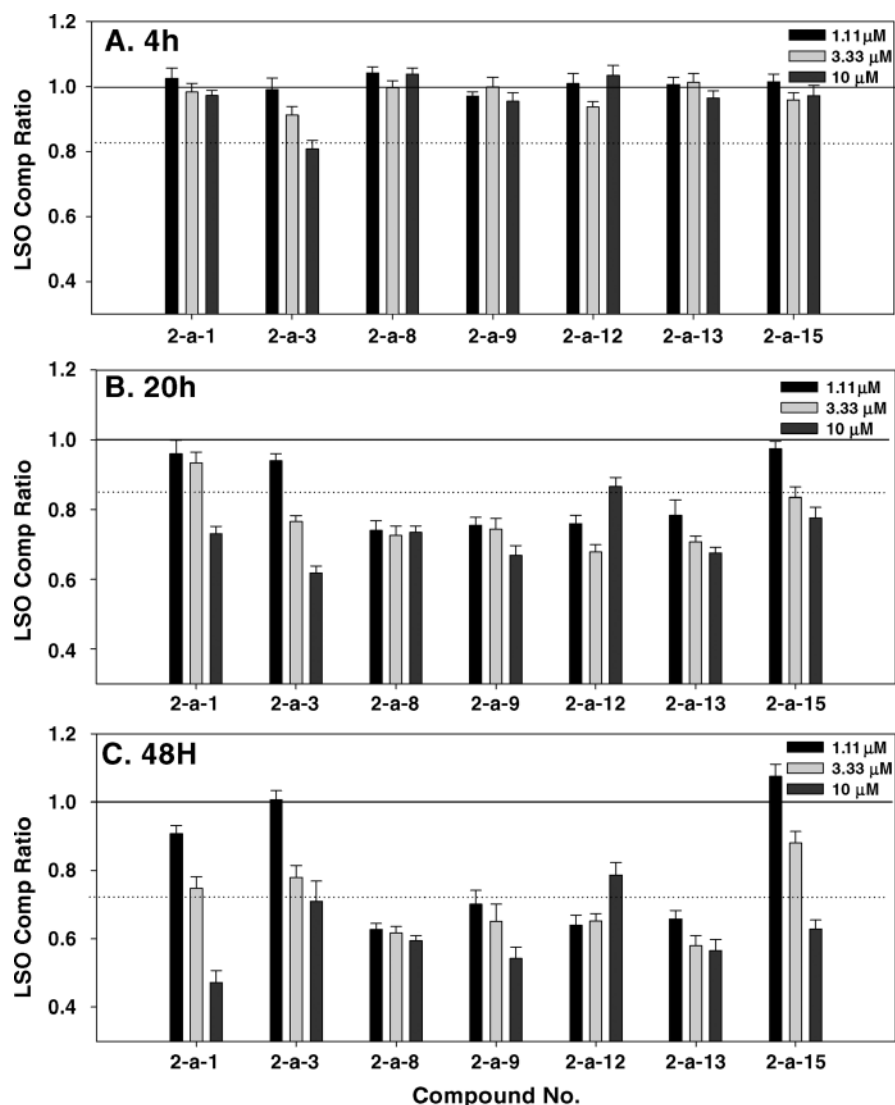


Fig. 11. Time course of effects of seven hit compounds from the secondary library. CT60 cells were seeded on 384-well plates in growth medium. After 24 h, compounds were added to achieve final concentrations of 1.11, 3.33, and 10 μ M in four different wells/concentration and allowed to incubate for 4 h (A), 20 h (B), and 48 h (C). Cells were washed with PBS, fixed with PFA, and stained with filipin. Images were obtained at 10 \times magnification using the Discovery-1 automated fluorescence microscope and 360/40 nm excitation and 480/40 nm emission filters equipped with a 365 DCLP filter. LSO compartment ratio was measured (average of three different experiments). The solid horizontal lines indicate mean values for the solvent control, and the dashed lines indicate means -3 SD. Error bars represent standard error.

the use of the automated microscopy analysis. First, the microscopy system is a very sensitive detector of the relatively weak filipin fluorescence. Second, we restricted the measurement to the areas in each field that contained cells, which reduced the contribution from background. Finally, dividing total fluorescence power by the area covered by cells provides a correction for differences in cell density at the time of measurement. We found that the filipin intensity per pixel provided enough discrimination of mutant versus wild-type cells to be useful as a preliminary screen. We used this parameter to optimize experimental conditions such as cell density and labeling conditions to be used in the assays.

The second assay, the LSO compartment ratio assay, used a second threshold to identify areas in each field that contained heavily labeled organelles, which are the LSOs in the mutant cells. Because these are the sites of cholesterol accumulation in NPC cells, it would be expected that selective measurement of this pool of cholesterol would provide better discrimination of mutant versus wild-type cells, and we found that this was the case.

Although we developed this assay for use in CHO cell lines, it should be applicable, with minor modifications, for analyzing cholesterol accumulation in other cell types. The development of an assay for cholesterol accumulation has potential use not only for NPC but also for other

TABLE 3. Summary of the effects of seven hit compounds from the secondary library on CT60 cells

Compound	Lowest Effective Dose (Lysosome-Like Storage Organelle Assay) – 3 SD at 20 h	Average Filipin Assay at 10 μ M Dose	μ g FC/ μ g Protein (GC) at 10 μ M Dose	Protein Content μ g/well	Cell Count after 24 h at 10 μ M Dose
2-a-1	3.33 μ M	0.74 \pm 0.02	0.65 \pm 0.02	0.94 \pm 0.03	1.00
2-a-3	3.33 μ M	0.75 \pm 0.01	0.81 \pm 0.03	0.92 \pm 0.04	1.00
2-a-8	123 nM	0.74 \pm 0.01	0.76 \pm 0.03	0.94 \pm 0.04	0.96
2-a-9	370 nM	0.74 \pm 0.01	0.75 \pm 0.04	0.94 \pm 0.05	0.90
2-a-12	370 nM	0.87 \pm 0.01	—	—	0.67
2-a-13	370 nM	0.75 \pm 0.02	0.79 \pm 0.04	0.97 \pm 0.03	1.00
2-a-15	3.33 μ M	0.79 \pm 0.01	0.89 \pm 0.03	0.84 \pm 0.02	0.94

Data are presented as fractions of solvent-treated controls.

glycolipid storage disorders. Although the underlying biochemical bases for the disorders vary, many of them result in a similar phenotype that includes the formation of internal membrane whorls in LSOs that contain sphingomyelin, BMP, and cholesterol (55). In Fig. 12, we show that the screening assay can be used to analyze cholesterol accumulation caused by the treatment of normal human fibroblasts with U18666A.

This assay can be used not only for chemical screens such as the one described here but also for molecular genetics screens such as RNA interference knockdown and gene expression. Using conventional methods, a few genes have been identified that can correct the NPC phenotype when overexpressed in cells (36, 38, 56). The screen we

have described here could be used for large-scale gene expression screens.

In the first round of screening of a diverse library of 14,956 compounds combinatorially synthesized from 126 templates, we found 14 compounds that caused a significant decrease in the filipin labeling at 10 μ M, including 3 compounds that produced significant reduction at 123 nM. Five of the selected compounds belong to one family, and two were from another family (Fig. 5). Our finding that several of the selected compounds were chemically related suggests that they may interact with the same molecular target in the cells.

We selected a secondary library chemically similar to these compounds. In screening the secondary library, we

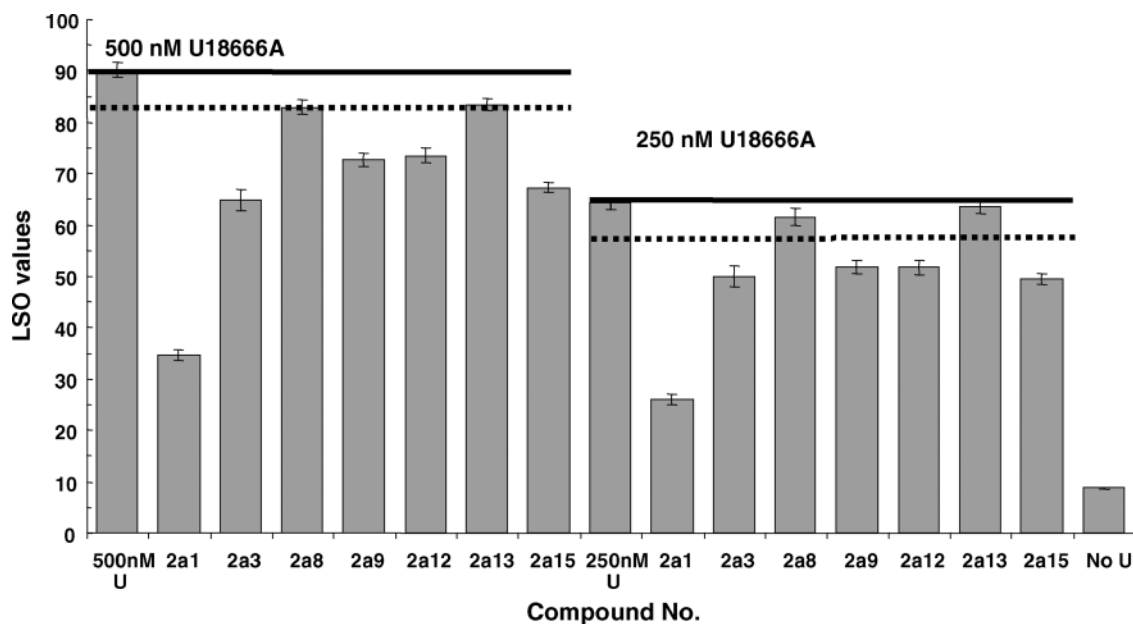


Fig. 12. Effects of seven hit compounds from the secondary library on 3- β -[2-diethylaminoethoxy]androst-5-17-one hydrochloride (U18666A)-treated normal human fibroblasts. Normal human fibroblasts were plated on 384-well plates and grown in regular growth medium for 24 h, after which the cells were treated with compound U18666A (500 or 250 nM) in screening medium for 4 h. The cells were then further incubated overnight with hit compounds (10 μ M) in the continued presence of U18666A. Finally, cells were washed three times with PBS, fixed with 1.5% PFA, washed again with PBS, and stained with filipin. Images were acquired using the Discovery-1 microscope at 10 \times magnification and analyzed for the LSO ratio. LSO ratio values shown in this figure were not normalized to a value from untreated control cells. The solid horizontal lines are means for U18666A-treated cells at each concentration, and the dotted horizontal lines are means – 3 SD. Error bars represent standard error.

used lower doses and also placed a greater emphasis on nontoxicity, because several of the selected compounds from the initial screen showed some toxicity. Even though we reduced the dose used for selecting compounds from 10 to 1 μ M, we obtained a higher fraction of selected compounds in the secondary library screen (0.18%) than in the initial screen (0.1%). Thus, the selection of chemicals in the secondary library led to a significant enrichment in potential hits. In the secondary library screening, we did not find compounds that were significantly effective at <120 nM, but several of the selected compounds had lower toxicity than the compounds from the initial screen.

The seven compounds selected for further characterization can generally be divided into two groups. Compounds 2-a-1, 2-a-9, 2-a-12, and 2-a-13 (group I) are based on a 1,3,5-triazine core, and this class of compounds has been of significant interest in the field of medicinal chemistry (57–61). The second group of compounds (group II) have five membered ring heterocycle cores (2-a-3 contains a 2-thioxo-1,3-thiazolidin-4-one derivative, 2-a-15 contains a methine-linked pyrrole and pyrrol-2-one, and 2-a-8 contains a 1,3-thiazole *N*-linked to a dihydropyrazole). Both groups of compounds are extensively substituted from the cores, with group I triazines bearing mostly aryl or cyclic amines (or bearing a hydrazino group). Group II compounds are also aryl-substituted, with compound 2-a-3 featuring an interesting partially saturated diethyl-amino benzene moiety connected to the 2-thioxo-1,3-thiazolidin-4-one via a double bond. Compound 2-a-15 has three aromatic rings in extended conjugation, whereas compound 2-a-8 incorporates six different ring systems, of which five are aromatic. Both group I and group II compounds appear to be highly conformationally restricted molecules with extensive unsaturation. Their peripheries tend to be very hydrophobic, whereas their centers are more hydrophilic. We note that this characteristic implies that they are a type of spatial amphiphile (hydrophobic outside, hydrophilic inside). Although there are hydrophilic groups at the peripheries in some cases (notably the 2-a-13 nitro group), the consistent distribution of several hydrogen bonding moieties to the cores of these structures suggests that the cores may assist specific recognition of their *in vivo* targets. An investigation of the specific structural features that give rise to the biological properties of these molecules is under way.

Six of the seven compounds selected in the secondary screen had low cytotoxicity and reduced FC significantly not only in LSOs but also in the whole cell. Several of these compounds were effective at concentrations of <0.5 μ M. Table 3 summarizes the effects of these six hit compounds from the secondary library in terms of cholesterol reduction as well as toxic effects.


In addition to the selection of cholesterol-lowering compounds, which was the goal of the screen, we found compounds that had other apparent effects. Some of the compounds were found to increase filipin staining even above the levels found in the NPC mutant cells. Some compounds that initially appeared to increase filipin staining were found to be fluorescent at wavelengths that

overlapped the spectrum of filipin, and their fluorescence was probably the basis for the increased fluorescence seen in the assay. However, several nonfluorescent compounds were also found to increase filipin staining in the NPC cells. In addition, we found some compounds that created a significant change in the morphology of the compartments that are enriched in FC. In particular, compound 1-b-4 produced a large network of apparently tubular organelles that were labeled with filipin.

The mechanisms of action of the compounds that partially reverse the NPC phenotype will require further investigation. It is thought that cholesterol efflux from late endosomes requires several steps and, like many steps of intracellular cholesterol transport, is apparently mainly nonvesicular (62). NPC2 presumably plays a role in delivering cholesterol from the sites of hydrolysis of sterol esters to the limiting membrane of the organelles (63). NPC1, and presumably other proteins, would facilitate the delivery of cholesterol from the limiting membrane to cytosolic carriers. These carriers, which have not been identified molecularly, would transport cholesterol to the plasma membrane or other organelles (64, 65). Total FC in the cells could be reduced by increasing efflux to extracellular acceptors via the plasma membrane and/or esterification of cholesterol by ACAT in the endoplasmic reticulum. Reduced uptake of cholesterol or reduced synthesis could also cause a reduction in cellular cholesterol during the incubation with compounds. We assayed for reduction of the lipid BMP, which accumulates in NPC cells (22), using an analysis method similar to the average intensity and LSO assays. None of the hit compounds from the secondary library produced a significant reduction in BMP labeling after 16 h incubations (data not shown). Several of the hit compounds from the secondary library did cause reductions in cholesterol accumulation in normal human fibroblasts treated with U18666A, which causes cholesterol accumulation in LSOs. This indicates that the compounds do not rely on the SCAP mutation or other special properties of the CHO cell lines used for the screen.

The compounds could directly affect the LSOs, but other indirect effects will also need to be considered. For example, overexpression of Rab4, a small GTPase that is normally associated with sorting endosomes or the endocytic recycling compartment, can partially correct the NPC phenotype (66). It is unclear how alterations of traffic in the early endosomes would affect cholesterol storage in LSOs, but such an effect of one of the compounds could indirectly alter cholesterol efflux or delivery to ACAT.

The compounds found in this screen are of sufficient potency to be useful for future studies aimed at identifying their sites of action. This could include modification of the compounds with photoreactive groups for labeling binding partners or linkage to biotin for affinity purification. Identification of binding partners will be necessary for a full understanding of the molecular mechanisms. In conclusion, the studies presented here show that small molecules added to cells can partially correct the NPC1 defect in cultured cells. Because several of these compounds are effective in reducing cholesterol accumulation

at concentrations at which they are nontoxic to cultured NPC1 cells, they have potential use as lead compounds for drug discovery. 

The authors thank Dr. T. Y. Chang (Dartmouth University) for providing CT60 and CT43 cell lines, Dr. J. Gruenberg (University of Geneva) for providing LBPA/BMP antibody, Drs. Charles Karan and Edward Hyde (High-Throughput Screening Facility, Rockefeller University) for assistance with the chemical libraries, and Inge Hanson and Dr. Richard Deckelbaum (Columbia University) for assistance with gas chromatography. We are grateful to Dr. Anthony Sauve (Weill-Cornell Medical College) for helpful discussions. This work was supported by National Institutes of Health Grant DK-27083 and by a grant from the Ara Parseghian Medical Research Foundation. M.R. was supported in part by a grant from the W. M. Keck Foundation.

REFERENCES

- Pentchev, P., M. T. Vanier, K. Suzuki, and M. C. Patterson. 1995. Niemann-Pick Disease Type C: Cellular Cholesterol Lipidosis. *In The Metabolic and Molecular Bases of Inherited Diseases*, 7th ed. C. R. Scriver, W. S. Sly, B. Childs, A. L. Beaudet, D. Valle, K.W. Kinzler, and B. Vogelstein, editors. McGraw-Hill, New York. 2625–2639.
- Li, H., J. J. Repa, M. A. Valasek, E. P. Beltray, S. D. Turley, D. C. German, and J. M. Dietschy. 2005. Molecular, anatomical, and biochemical events associated with neurodegeneration in mice with Niemann-Pick type C disease. *J. Neuropathol. Exp. Neurol.* **64**: 323–333.
- Patterson, M. C., and F. Platt. 2004. Therapy of Niemann-Pick disease, type C. *Biochim. Biophys. Acta.* **1685**: 77–82.
- Hsich, G., M. Sena-Esteves, and X. O. Breakefield. 2002. Critical issues in gene therapy for neurologic disease. *Hum. Gene Ther.* **13**: 579–604.
- Liscum, L., E. Arnio, M. Anthony, A. Howley, S. L. Sturley, and M. Agler. 2002. Identification of a pharmaceutical compound that partially corrects the Niemann-Pick C phenotype in cultured cells. *J. Lipid Res.* **43**: 1708–1717.
- Bascunan-Castillo, E. C., R. P. Erickson, C. M. Howison, R. J. Hunter, R. H. Heidenreich, C. Hicks, T. P. Trouard, and R. J. Gillies. 2004. Tamoxifen and vitamin E treatments delay symptoms in the mouse model of Niemann-Pick C. *J. Appl. Genet.* **45**: 461–467.
- Zervas, M., K. L. Somers, M. A. Thrall, and S. U. Walkley. 2001. Critical role for glycosphingolipids in Niemann-Pick disease type C. *Curr. Biol.* **11**: 1283–1287.
- Griffin, L. D., W. Gong, L. Verot, and S. H. Mellon. 2004. Niemann-Pick type C disease involves disrupted neurosteroidogenesis and responds to allopregnanolone. *Nat. Med.* **10**: 704–711.
- Vanier, M. T., and K. Suzuki. 1998. Recent advances in elucidating Niemann-Pick C disease. *Brain Pathol.* **8**: 163–174.
- Goldstein, J. L., and M. S. Brown. 1992. Lipoprotein receptors and the control of plasma LDL cholesterol levels. *Eur. Heart J.* **13** (Suppl. B): 34–36.
- Garver, W. S., and R. A. Heidenreich. 2002. The Niemann-Pick C proteins and trafficking of cholesterol through the late endosomal/lysosomal system. *Curr. Mol. Med.* **2**: 485–505.
- Carstea, E. D., J. A. Morris, K. G. Coleman, S. K. Loftus, D. Zhang, C. Cummings, J. Gu, M. A. Rosenfeld, W. J. Pavan, D. B. Krizman, et al. 1997. Niemann-Pick C1 disease gene: homology to mediators of cholesterol homeostasis. *Science.* **277**: 228–231.
- Liscum, L. 2000. Niemann-Pick type C mutations cause lipid traffic jam. *Traffic.* **1**: 218–225.
- Puri, V., R. Watanabe, M. Dominguez, X. Sun, C. L. Wheatley, D. L. Marks, and R. E. Pagano. 1999. Cholesterol modulates membrane traffic along the endocytic pathway in sphingolipid-storage diseases. *Nat. Cell Biol.* **1**: 386–388.
- Ioannou, Y. A. 2000. The structure and function of the Niemann-Pick C1 protein. *Mol. Genet. Metab.* **71**: 175–181.
- Scott, C., and Y. A. Ioannou. 2004. The NPC1 protein: structure implies function. *Biochim. Biophys. Acta.* **1685**: 8–13.
- Vanier, M. T., and G. Millat. 2004. Structure and function of the NPC2 protein. *Biochim. Biophys. Acta.* **1685**: 14–21.
- Friedland, N., H. L. Liou, P. Lobel, and A. M. Stock. 2003. Structure of a cholesterol-binding protein deficient in Niemann-Pick type C2 disease. *Proc. Natl. Acad. Sci. USA.* **100**: 2512–2517.
- Okamura, N., S. Kiuchi, M. Tamba, T. Kashima, S. Hiramoto, T. Baba, F. Dacheux, J. L. Dacheux, Y. Sugita, and Y. Z. Jin. 1999. A porcine homolog of the major secretory protein of human epididymis, HE1, specifically binds cholesterol. *Biochim. Biophys. Acta.* **1438**: 377–387.
- Zhang, M., M. Sun, N. K. Dwyer, M. E. Comly, S. C. Patel, R. Sundaram, J. A. Hanover, and E. J. Blanchette-Mackie. 2003. Differential trafficking of the Niemann-Pick C1 and 2 proteins highlights distinct roles in late endocytic lipid trafficking. *Acta Paediatr. Suppl.* **92**: 63–73.
- Sun, X., D. L. Marks, W. D. Park, C. L. Wheatley, V. Puri, J. F. O'Brien, D. L. Kraft, P. A. Lundquist, M. C. Patterson, R. E. Pagano, et al. 2001. Niemann-Pick C variant detection by altered sphingolipid trafficking and correlation with mutations within a specific domain of NPC1. *Am. J. Hum. Genet.* **68**: 1361–1372.
- Kobayashi, T., M. H. Beuchat, M. Lindsay, S. Frias, R. D. Palmiter, H. Sakuraba, R. G. Parton, and J. Gruenberg. 1999. Late endosomal membranes rich in lysobisphosphatidic acid regulate cholesterol transport. *Nat. Cell Biol.* **1**: 113–118.
- Mukherjee, S., and F. R. Maxfield. 2004. Lipid and cholesterol trafficking in NPC. *Biochim. Biophys. Acta.* **1685**: 28–37.
- Bornig, H., and G. Geyer. 1974. Staining of cholesterol with the fluorescent antibiotic "filipin." *Acta Histochem.* **50**: 110–115.
- Maxfield, F. R., and D. Wustner. 2002. Intracellular cholesterol transport. *J. Clin. Invest.* **110**: 891–898.
- Lange, Y., J. Ye, and T. L. Steck. 1998. Circulation of cholesterol between lysosomes and the plasma membrane. *J. Biol. Chem.* **273**: 18915–18922.
- Chen, W., Y. Sun, C. Welch, A. Gorelik, A. R. Leventhal, I. Tabas, and A. R. Tall. 2001. Preferential ATP-binding cassette transporter A1-mediated cholesterol efflux from late endosomes/lysosomes. *J. Biol. Chem.* **276**: 43564–43569.
- Pentchev, P. G., M. E. Comly, H. S. Kruth, M. T. Vanier, D. A. Wenger, S. Patel, and R. O. Brady. 1985. A defect in cholesterol esterification in Niemann-Pick disease (type C) patients. *Proc. Natl. Acad. Sci. USA.* **82**: 8247–8251.
- Lin, S., X. Lu, C. C. Chang, and T. Y. Chang. 2003. Human acyl-coenzyme A:cholesterol acyltransferase expressed in Chinese hamster ovary cells: membrane topology and active site location. *Mol. Biol. Cell.* **14**: 2447–2460.
- Park, W. D., J. F. O'Brien, P. A. Lundquist, D. L. Kraft, C. W. Vockley, P. S. Karnes, M. C. Patterson, and K. Snow. 2003. Identification of 58 novel mutations in Niemann-Pick disease type C: correlation with biochemical phenotype and importance of PTCL-like domains in NPC1. *Hum. Mutat.* **22**: 313–325.
- Yang, C. C., Y. N. Su, P. C. Chiou, M. J. Fietz, C. L. Yu, W. L. Hwu, and M. J. Lee. 2005. Six novel NPC1 mutations in Chinese patients with Niemann-Pick disease type C. *J. Neurol. Neurosurg. Psychiatry.* **76**: 592–595.
- Vanier, M. T., and G. Millat. 2003. Niemann-Pick disease type C. *Clin. Genet.* **64**: 269–281.
- Di Leo, E., F. Panico, P. Tarugi, C. Battisti, A. Federico, and S. Calandra. 2004. A point mutation in theariat branch point of intron 6 of NPC1 as the cause of abnormal pre-mRNA splicing in Niemann-Pick type C disease. *Hum. Mutat.* **24**: 440.
- Patterson, M. C., M. T. Vanier, K. Suzuki, J. A. Morris, E. Cartsea, E. B. Neufeld, E. J. Blanchette-Mackie, and P. G. Pentchev. 2001. Niemann-Pick type C: a lipid trafficking disorder. *In The Metabolic and Molecular Bases of Inherited Disease*. B. A. Scriver, D. Valle, W. S. Sly, B. Childs, K. W. Kinzler, and B. Vogelstein, editors. McGraw Hill, New York. 3611–3633.
- Meiner, V., S. Shpitz, H. Mandel, A. Klar, Z. Ben-Neriah, J. Zlotogora, M. Sagi, A. Lossos, R. Bargal, V. Sury, et al. 2001. Clinical-biochemical correlation in molecularly characterized patients with Niemann-Pick type C. *Genet. Med.* **3**: 343–348.
- Choudhury, A., M. Dominguez, V. Puri, D. K. Sharma, K. Narita, C. L. Wheatley, D. L. Marks, and R. E. Pagano. 2002. Rab proteins mediate Golgi transport of caveola-internalized glycosphingolipids and correct lipid trafficking in Niemann-Pick C cells. *J. Clin. Invest.* **109**: 1541–1550.

37. Blom, T. S., M. D. Linder, K. Snow, H. Pihko, M. W. Hess, E. Jokitalo, V. Veckman, A. C. Syvanen, and E. Ikonen. 2003. Defective endocytic trafficking of NPC1 and NPC2 underlying infantile Niemann-Pick type C disease. *Hum. Mol. Genet.* **12**: 257–272.
38. Walter, M., J. P. Davies, and Y. A. Ioannou. 2003. Telomerase immortalization upregulates Rab9 expression and restores LDL cholesterol egress from Niemann-Pick C1 late endosomes. *J. Lipid Res.* **44**: 243–253.
39. Maxfield, F. R., and T. E. McGraw. 2004. Endocytic recycling. *Nat. Rev. Mol. Cell Biol.* **5**: 121–132.
40. Mukherjee, S., and F. R. Maxfield. 2004. Membrane domains. *Annu. Rev. Cell Dev. Biol.* **20**: 839–866.
41. Prinz, W. 2002. Cholesterol trafficking in the secretory and endocytic systems. *Semin. Cell Dev. Biol.* **13**: 197–203.
42. Cruz, J. C., S. Sugii, C. Yu, and T. Y. Chang. 2000. Role of Niemann-Pick type C1 protein in intracellular trafficking of low density lipoprotein-derived cholesterol. *J. Biol. Chem.* **275**: 4013–4021.
43. Pitas, R. E., T. L. Innerarity, J. N. Weinstein, and R. W. Mahley. 1981. Acetoacetylated lipoproteins used to distinguish fibroblasts from macrophages in vitro by fluorescence microscopy. *Arteriosclerosis*. **1**: 177–185.
44. Dunn, K. W., and F. R. Maxfield. 1992. Delivery of ligands from sorting endosomes to late endosomes occurs by maturation of sorting endosomes. *J. Cell Biol.* **117**: 301–310.
45. Decker, T., and M. L. Lohmann-Matthes. 1988. A quick and simple method for the quantitation of lactate dehydrogenase release in measurements of cellular cytotoxicity and tumor necrosis factor (TNF) activity. *J. Immunol. Methods*. **115**: 61–69.
46. Shiratori, Y., A. K. Okwu, and I. Tabas. 1994. Free cholesterol loading of macrophages stimulates phosphatidylcholine biosynthesis and up-regulation of CTP:phosphocholine cytidylyltransferase. *J. Biol. Chem.* **269**: 11337–11348.
47. Lowry, O. H., N. J. Rosebrough, A. L. Farr, and R. J. Randall. 1951. Protein measurement with the Folin phenol reagent. *J. Biol. Chem.* **193**: 265–275.
48. McGraw, T. E., L. Greenfield, and F. R. Maxfield. 1987. Functional expression of the human transferrin receptor cDNA in Chinese hamster ovary cells deficient in endogenous transferrin receptor. *J. Cell Biol.* **105**: 207–214.
49. Zhang, J. H., T. D. Chung, and K. R. Oldenburg. 1999. A simple statistical parameter for use in evaluation and validation of high throughput screening assays. *J. Biomol. Screen.* **4**: 67–73.
50. Willet, P., B. JM., Down, GM. 1998. Chemical similarity searching. *J. Chem. Inf. Comput. Sci.* **38**: 983–996.
51. Hua, X., A. Nohturfft, J. L. Goldstein, and M. S. Brown. 1996. Sterol resistance in CHO cells traced to point mutation in SREBP cleavage-activating protein. *Cell*. **87**: 415–426.
52. Chang, T. Y., and J. S. Limanek. 1980. Regulation of cytosolic acetoacetyl coenzyme A thiolase, 3-hydroxy-3-methylglutaryl coenzyme A synthase, 3-hydroxy-3-methylglutaryl coenzyme A reductase, and mevalonate kinase by low density lipoprotein and by 25-hydroxycholesterol in Chinese hamster ovary cells. *J. Biol. Chem.* **255**: 7787–7795.
53. Jacobs, N. L., B. Andemariam, K. W. Underwood, K. Panchalingam, D. Sternberg, M. Kielian, and L. Liscum. 1997. Analysis of a Chinese hamster ovary cell mutant with defective mobilization of cholesterol from the plasma membrane to the endoplasmic reticulum. *J. Lipid Res.* **38**: 1973–1987.
54. Zhang, M., N. K. Dwyer, E. B. Neufeld, D. C. Love, A. Cooney, M. Comly, S. Patel, H. Watari, J. F. Strauss 3rd, P. G. Pentchev, et al. 2001. Sterol-modulated glycolipid sorting occurs in Niemann-Pick C1 late endosomes. *J. Biol. Chem.* **276**: 3417–3425.
55. Boven, L. A., M. van Meurs, R. G. Boot, A. Mehta, L. Boon, J. M. Aerts, and J. D. Laman. 2004. Gaucher cells demonstrate a distinct macrophage phenotype and resemble alternatively activated macrophages. *Am. J. Clin. Pathol.* **122**: 359–369.
56. Neufeld, E. B., J. A. Stonik, S. J. Demosky, Jr., C. L. Knapper, C. A. Combs, A. Cooney, M. Comly, N. Dwyer, J. Blanchette-Mackie, A. T. Remaley, et al. 2004. The ABCA1 transporter modulates late endocytic trafficking: insights from the correction of the genetic defect in Tangier disease. *J. Biol. Chem.* **279**: 15571–15578.
57. Brzozowski, Z. 1998. 2-Mercapto-N-(azoly)benzenesulfonamides. V. Syntheses, anti-HIV and anticancer activity of some 4-chloro-2-mercapto-5-methyl-N-(1,2,4-triazolo[4,3-a]pyrid-3-yl)benzenesulfonamides. *Acta Pol. Pharm.* **55**: 375–379.
58. Brzozowski, Z., F. Saczewski, and M. Gdaniec. 2000. Synthesis, structural characterization and antitumor activity of novel 2,4-diamino-1,3,5-triazine derivatives. *Eur. J. Med. Chem.* **35**: 1053–1064.
59. Schatzberg, A. F. 2004. Employing pharmacologic treatment of bipolar disorder to greatest effect. *J. Clin. Psychiatry*. **65 (Suppl. 15)**: 15–20.
60. Mohr, R., A. Buschauer, and W. Schunack. 1986. H₂-antihistaminics. 31. 1,2,5-Triazine-2,4-diamines and -2,4,6-triamines with H₂-antagonistic activity. *Arch. Pharm. (Weinheim)*. **319**: 878–885.
61. Chambers, M. S., J. R. Atack, R. W. Carling, N. Collinson, S. M. Cook, G. R. Dawson, P. Ferris, S. C. Hobbs, D. O'Connor, G. Marshall, et al. 2004. An orally bioavailable, functionally selective inverse agonist at the benzodiazepine site of GABA α 5 receptors with cognition enhancing properties. *J. Med. Chem.* **47**: 5829–5832.
62. Hao, M., S. X. Lin, O. J. Karylowski, D. Wustner, T. E. McGraw, and F. R. Maxfield. 2002. Vesicular and non-vesicular sterol transport in living cells. The endocytic recycling compartment is a major sterol storage organelle. *J. Biol. Chem.* **277**: 609–617.
63. Sleat, D. E., J. A. Wiseman, M. El-Banna, S. M. Price, L. Verot, M. M. Shen, G. S. Tint, M. T. Vanier, S. U. Walkley, and P. Lobel. 2004. Genetic evidence for nonredundant functional cooperativity between NPC1 and NPC2 in lipid transport. *Proc. Natl. Acad. Sci. USA*. **101**: 5886–5891.
64. Strauss, J. F., 3rd, T. Kishida, L. K. Christenson, T. Fujimoto, and H. Hiroi. 2003. START domain proteins and the intracellular trafficking of cholesterol in steroidogenic cells. *Mol. Cell. Endocrinol.* **202**: 59–65.
65. Tall, A. R. 2003. Role of ABCA1 in cellular cholesterol efflux and reverse cholesterol transport. *Arterioscler. Thromb. Vasc. Biol.* **23**: 710–711.
66. Choudhury, A., D. K. Sharma, D. L. Marks, and R. E. Pagano. 2004. Elevated endosomal cholesterol levels in Niemann-Pick cells inhibit rab4 and perturb membrane recycling. *Mol. Biol. Cell*. **15**: 4500–4511.